A vibrational spectroscopic study of a hydrated hydroxy-phosphate mineral fluellite, $Al_2(PO_4)F_2(OH)\cdot 7H_2O$

Jiří Čejka,[1,2] Jiří Sejkora,[1] Ivo Macek,[1] Ray L. Frost,[2•], Andrés López,[2] Ricardo Scholz,[3] Yunfei Xi,[2]

[1] Department of Mineralogy and Petrology, National Museum, Cirkusová 1740, CZ-193 00, Praha 9, Czech Republic.

[2] School of Chemistry, Physics and Mechanical Engineering, Science and Engineering Faculty, Queensland University of Technology, GPO Box 2434, Brisbane Queensland 4001, Australia.

[3] Geology Department, School of Mines, Federal University of Ouro Preto, Campus Morro do Cruzeiro, Ouro Preto, MG, 35,400-00, Brazil

ABSTRACT

Raman and infrared spectra of two well-defined fluellite samples, $Al_2(PO_4)F_2(OH).7H_2O$, from the Krásno near Horní Slavkov (Czech Republic) and Kapunda, South Australia (Australia) were studied and tentatively interpreted. Observed bands were assigned to the stretching and bending vibrations of phosphate tetrahedra, aluminum oxide/hydroxide/fluoride octahedra, water molecules and hydroxyl ions. Approximate O-H···O hydrogen bond lengths were inferred from the Raman and infrared spectra.

KEYWORDS: fluellite, phosphate, hydroxyl ions, Raman spectroscopy, infrared spectroscopy

• Author to whom correspondence should be addressed (r.frost@qut.edu.au)

INTRODUCTION

Fluellite $Al_2(PO_4)F_2(OH).7H_2O$ is very rare, late hydrothermal or supergene mineral formed by alteration of earlier phosphates minerals. It may be found as a colourless to purple-black crystals [1] but usually forms a colorless to white and yellow crystals or powder aggregates in association with fluorapatite, wavellite, cacoxenite, variscite, strengite, minyulite etc. The size of the crystals is several mm rare up to 1 cm [2]. It occurs in several types of geological environments, for example in complex granitic pegmatites [3-4], phosphatic marbles [5], in lateritic conglomerate and phosphatic sedimentary rocks [6-8] and at ore deposits [1,9-11].

Fluellite was described as a new mineral in 1824 by Lévy [12] without any quantitative chemical tests only with presence of aluminum and fluorine. Further chemical data were presented in 1882 by Groth [13] and proposed the formula $AlF_8 . H_2O$. In 1920 Laubmann and Steinmetz [14] described mineral kreuzbergite from Oberpfalz, Bavaria as an aluminium phosphate. These two minerals with similar compositions existed till 1940 when Scholz and Strunz [15] carried out qualitative chemical analyses on kreuzbergite and concluded that it has the same composition as fluellite. The name kreuzbergite was discredited and only fluellite remained.

The mineral fluellite has orthorombic symmetry with space group Fddd. Its crystal structure was solved by Guy et al. [16-17] and consists of octahedrally [Al-O] and tetrahedrally $[PO_4]$ coordinated cations in open framework arrangement within which there are distinct channels containing hydrogen-bonded water molecules. The aluminium atoms are situated at centers of symmetry and are bonded octahedrally to two centro-symmetric pairs of oxygen atoms and one pair of fluorine ions. Raman spectrum of fluellite from Gold Quarry mine, Maggie Creek District, Eureka County, Nevada (U.S.A.) was published in the RRUFF's data base (fluellite R070473) without any resolution of band wavenumbers and assignment.

The aim of this paper is to report the Raman spectra of well-defined natural hydrated phosphate minerals, fluellite from two different occurrences, and to relate the spectra to this molecular and the crystal structure. The paper follows the systematic research of the large group of oxyanion containig minerals [18-21], and especially their molecular structure using IR and Raman spectroscopy [22-25].

EXPERIMENTAL

Minerals

The studied samples of the mineral fluellite originated from two different occurrences: greisen Sn-W deposit Krásno near Horní Slavkov [2], western Bohemia, Czech Republic (labelled as CZ) and phosphate deposit Kapunda [26], Mt. Lofty Ranges, South Australia, Australia (labelled as AU). At both occurrences, fluellite forms very brittle, water-clear translucent dipyramidal crystals up to 1 cm (CZ) or only 1 mm in size (AU).

Carefully hand-picked samples were used for X-ray powder diffraction experiments. To minimize the complicated shape of background, the samples studied were placed on a flat low-background silicon wafer. Powder XRD measurements were carried out with CuKα radiation at a HZG4/Arem diffractometer (50 kV, 40 mA) in the range 5-70^{o} 2θ in the step-scan mode 0.02^{o}/5 s (CZ) and at a Bruker D8 Advance diffractometer (40 kV, 40 mA) in the range 5-70 ^{o} 2θ in the step-scan mode 0.01^{o}/8 s (AU). The position and intensities of reflections were calculated using the Pearson VII profile shape function in the ZDS program package [27]. The measured patterns were indexed using theoretical pattern calculated from the crystal-structure data of fluellite [16-17]. The unit-cell parameters refined from measured powder XRD using the program of Burnham [28] are compared with published data in the Table 1.

The fluellite sample (CZ) was quantitatively analysed by Cameca SX 100 electron microprobe system in wavelength dispersion mode for chemical composition. Studied sample was mounted into the epoxide resin and polished. The polished surface was coated with carbon layer 250 Å. An acceleration voltage of 15 kV, a specimen current of 10 nA, and a beam diameter of 5 μm were used. Well-defined natural and synthetic compounds were used as standards. The raw intensities were converted to the concentrations using automatic *PAP* matrix correction software package. The calculation of theoretical content of H_2O corresponding to ideal formula provided the totals near 120 wt. % (Table 2); it indicates a strong dehydratation, corresponding to loss of two H_2O molecules during sample coating in vacuum and analysis. This loss is indicated by irregular fracturing of the analyzes samples [2]. On the basis of 14 (O,OH,F), empirical formula of fluellite from Krásno may be expressed as $Al_{1.98}(PO_4)_{1.07}F_{1.99}(OH)_{0.75}.7H_2O$. Chemical composition of Kapunda fluellite (AU) was check by ED spectrum at the same EMPA, obtained ED spectra for both samples (CZ,AU) are practically identical, only very minor Fe content was found at AU sample.

Raman and infrared spectroscopy

Fragments of single crystals of fluellite were placed on a polished metal surface on the stage of an Olympus BHSM microscope, which is equipped with 10x, 20x, and 50x objectives. The microscope is part of a Renishaw 1000 Raman microscope system, which also includes a monochromator, a filter system and a CCD detector (1024 pixels). The Raman spectra were excited by a Spectra-Physics model 127 He-Ne laser producing highly polarised light at 633 nm and collected at a nominal resolution of 2 cm^{-1} and a precision of ± 1 cm^{-1} in the range between 200 and 4000 cm^{-1}. Repeated acquisition on the crystals using the highest magnification (50x) were accumulated to improve the signal to noise ratio in the spectra. Spectra were calibrated using the 520.5 cm^{-1} line of a silicon wafer. Previous studies by the authors provide more details of the experimental technique. Alignment of all crystals in a similar orientation has been attempted and achieved. However, differences in intensity may be observed due to minor differences in the crystal orientation.

Infrared spectrum of fluellite sample from Kapunda was recorded by micro diffuse reflectance method (DRIFTS) on a Nicolet Magna 760 FTIR spectrometer (range 4000-600 cm^{-1}, resolution 4 cm^{-1}, 128 scans, 2 level zero-filtering, Happ-Genzel apodization), equipped with Spectra Tech InspectIR micro FTIR accessory. Sample of amount less than 0.050 mg was mixed without using pressure with KBr. Samples were immediately recorded together with the same KBr as a reference.

Spectral manipulation such as baseline correction/adjustment and smoothing were performed using the Spectracalc software package GRAMS (Galactic Industries Corporation, NH, USA). Band component analysis was undertaken using the Jandel 'Peakfit' software package that enabled the type of fitting function to be selected and allows specific parameters to be fixed or varied accordingly. Band fitting was done using a Lorentzian-Gaussian cross-product function with the minimum number of component bands used for the fitting process. The Gaussian-Lorentzian ratio was maintained at values greater than 0.7 and fitting was undertaken until reproducible results were obtained with squared correlations of r^2 greater than 0.995.

RESULTS AND DISCUSSION

Crystal symmetry and vibrational spectra of fluellite

Fluellite, $Al_2PO_4F_2(OH).7H_2O$, is orthorhombic, space group $Fddd - D_{2h}^{24}$, $Z = 8$. The structure consists of $AlF_2O_4.H_{3.5}$ octahedra linked through (PO_4) tetrahedra forming channels which contain the remaining water molecules. The water molecules and hydroxyl ions are hydrogen bonded. Two oxygen atoms in the Al^{3+} octahedra are shared with the (PO_4) tetrahedra. The other two are statistically one quater that of a hydroxyl ion and three quaters that of a water molecule [16-17]. According to Nakamoto [29], octahedral units XY_6 exhibit six normal vibrations ν_1 (A_{1g}) and ν_2 (E_g) stretching and ν_5 (F_{2g}) bending vibrations are Raman active, while only ν_3 (F_{1u}) stretching and ν_4 (F_{1u}) bending vibrations are infrared active. Symmetry lowering in the case of XY_4Z_2 may cause RA and IR activation of corresponding vibrations and also splitting of degenerate vibrations. Free $(PO_4)^{3-}$ anion exhibits tetrahedral T_d symmetry. In the case of a free ion of T_d symmetry, there are 9 normal vibration characterized by four fundamental distinguishable modes of vibrations: ν_1 (A_1) symmetric stretching vibration, Raman active, ν_2 (δ) (E) doubly degenerate bending vibration, Raman active, ν_3 (F_2) triply degenerate antisymmetric stretching vibration, Raman and infrared active, ν_4 (δ) (F_2) triply degenerate bending vibration, Raman and infrared active. T_d symmetry lowering may cause IR activation of the ν_1 and ν_2 vibrations and splitting of the doubly degenerate ν_2 and triply degenerate ν_3 and ν_4 vibrations. [29-30]. An overlap of stretching and bending vibrations of $AlO(OH)F_2$ octahedra with stretching and especially with bending vibrations of $(PO_4)^{3-}$ tetrahedra vibrations are supposed. Two fluellite samples were investigated, one sample from the Krásno, Czech Republic (CZ) and one from Kapunda, Australia (AU). RRUFF Raman spectrum of fluellite (specimen R070473 – Gold Quarry mine, Maggie Creek District, Eureka County, Nevada, U.S.A.) (cm^{-1}): 1120, 1096, 1038, 910, 651, 585, 524, 462, 406, 313, 276, 211, 173 (Figure S1). As usually, no interpretation of this spectrum was presented. Tentative assignment and intepretation of the Raman and infrared spectra of fluellite (Table 3) is realized with special regard to [29-33].

Raman and infrared spectroscopy

The Raman spectra of fluellite samples in the 100 to 4000 cm^{-1} spectral range are illustrated in Figures 1a,b. These spectra show the position of the Raman bands and their relative intensities. It is obvious that there are large parts of the spectrum where little or no intensity is observed. Therefore, the spectrum is subdivided into sections according to the type of vibration is being investigated. In this way the precise position of the bands can be detailed. The infrared spectrum of fluellite (AU) in the 500 to 4000 cm^{-1} spectral range is

shown in Figure 1c. As for the Raman spectrum, the infrared spectrum is subdivided into sections depending upon the type of vibration being examined. The complete infrared spectrum displays the position of the infrared bands and their relative intensity.

Raman and infrared region of ν OH stretching vibrations is presented in Figures 2a-c. Raman band at 3667 cm^{-1} (CZ) and infrared bands 3629 and 3559 cm^{-1} (AU) are assigned to the ν OH stretching vibrations of weakly hydrogen bonded hydroxyls, $(OH)^-$. Raman bands at 3396, 3314 and 3124 cm^{-1} (CZ) and 3411, 3356, 3222 and 3113 cm^{-1} (AU) and infrared bands at 3441, 3221 and 3047 cm^{-1} (AU) are attributed to the ν OH stretching vibrations of hydrogen bonded, structurally (symmetrically) distinct water molecules. Hydrogen bond lengths, O-H···O, vary approximately in the range from ~3.2 to ~2.67 Å [34].

Raman bands at 1670 cm^{-1} (CZ) and 1675 and 1603 cm^{-1} (AU) and infrared bands at 1660 and 1624 cm^{-1} (AU) (Figures 3a-c) are connected with ν_2 (δ) bending vibrations of structurally nonequivalent water molecules. Raman bands at 1583 cm^{-1} (CZ) and 1503 cm^{-1} (AU) and infrared bands at 1575 cm^{-1} and 1537 cm^{-1} (AU) may probably be assigned to overtones or combination bands.

The Raman spectra of fluellite in the 800(900) to 1200 cm^{-1} spectral range is reported in Figures 4a-b. The Raman spectra are dominated an intense band at 1036 cm^{-1} (CZ) and 1037 cm^{-1} (AU) and the infrared spectrum (Figure 4c) an weak band at 1026 cm^{-1} (AU) assigned to the ν_1 PO_4^{3-} symmetric stretching vibration. The Raman spectrum reported in this paper is in harmony with the spectrum provided in the RRUFF data base. The RRUFF spectrum shows an intense sharp band at 1038 cm^{-1}. The Raman spectra (Figures 4a-b) show resolved component bands at 1122 and 1096 cm^{-1} (CZ) and 1123, 1083 and 1061 cm^{-1} (AU) together with the infrared spectrum (AU) those at 1224, 1175, 1102 and a strong band at 1061 cm^{-1}. RRUFF Raman spectrum exhibits bands at 1120 and 1096 cm^{-1}. All these bands are assigned to the ν_3 PO_4^{3-} antisymmetric stretching vibrations. There is also a weak Raman band at 1003 cm^{-1} (AU), which may probably be a shoulder to the very intensive band of the ν_1 $(PO_4)^{3-}$ vibration or the δ Al-OH bending vibration. In the Raman spectrum of fluellite (AU) two low intensity component bands are observed at 963 and 926 cm^{-1}, which are related to the infrared bands (AU) at 965 and 920 cm^{-1}. These bands together with the Raman bands (CZ) at 897 and 835 cm^{-1} may be attributed to the Al-OH bending modes or to libration modes of water molecules. Normally the intensity of hydroxyl deformation modes are of a quite low intensity in the Raman spectrum but may show significantly greater intensity in the infrared spectrum. In the RRUFF Raman spectrum two broadish weak bands were observed

at around 880 and 910 cm^{-1}. It is suggested that these two bands may be due to hydroxyl deformation modes of the AlOH units. However, weak Raman bands at 897 and 835 cm^{-1} (CZ) could be also related to libration modes of water molecules as mentioned.

The infrared spectrum of fluellite in the 850 to 1300 cm^{-1} spectral range is shown in Figure 4c and shows much greater complexity than the Raman spectra. It is noted that the two infrared bands at 920 and 965 cm^{-1} attributed to the water librational modes show much greater intensity. Weak infrared bands was found at 1026 cm^{-1}, which is attributed to the ν_1 (PO_4) symmetric stretching vibrations and a strong band at 1061 cm^{-1} accompanied with some related weaker bands/shoulders at 1102, 1175 and 1224 cm^{-1} may be assigned to the split triply degenerate ν_3 $(PO_4)^{3-}$ antisymmetric stretching modes.

The Raman spectra of fluellite in the 350(400) to 700 cm^{-1} spectral range and in the 100 to 350(400) cm^{-1} spectral range are displayed in Figures 5a-b and 6a-b. Raman bands are observed at 646, 588, 557, 525 and 513 cm^{-1} (CZ) and 638, 614, 588, 522 and 510 cm^{-1} (AU) [RRUFF 651, 585, 524 cm^{-1}] are assigned to the ν_4 out of the plane bending modes of the $(PO_4)^{3-}$ units. Some overlap of these bands especially in the range from 585 to 646 cm^{-1} with the ν $Al(O,OH,F)_6$ octahedra stretching vibrations may be expected [32]. Raman bands 459 and 410 cm^{-1} (CZ) and 410 cm^{-1} (AU) [RRUFF 462 and 406 cm^{-1}] are observed. These bands are attributed to the ν_2 $(PO_4)^{3-}$ bending modes. Raman bands at 342 and 311 cm^{-1} (CZ) and 399 and 360 cm^{-1} (AU) [RRUFF 313 cm^{-1}] may be assigned to the ν $Al(O(OH)F)_6$ stretching vibrations. Strong Raman bands are observed at 295, 279 and 251 cm^{-1} (CZ), 297, 279, 258 and 249 cm^{-1} (AU) [RRUFF 276 cm^{-1}] are related to the O-Al-O skeletal stretching vibrations. Other Raman bands for fluellite samples studied are observed at 220, 208, 199, 191, 173, 151, 139, 123, 116, 108 cm^{-1} (CZ) and 194, 153, 141 and 113 cm^{-1} [RRUFF 211 and 173 cm^{-1}]. These bands are described as lattice vibrations.

CONCLUSIONS

1. Raman and infrared spectra of two well defined fluellite samples were recorded.
2. Observed Raman and infrared bands are tentatively intepreted and assigned to the stretching and bending vibrations of $(PO_4)^{3-}$ tetrahedra and (AlO_4F_2) octahedra, and of vibrations of hydrogen bonded water molecules and hydroxyl ions.

3. Approximate O-H···O hydrogen bond lengths are inferred from observed Raman and infrared bands connected with the ν OH stretching vibrations of water molecules and hydroxyl ions.

Acknowledgements

The financial and infra-structure support of the Queensland University of Technology Inorganic Materials Research Program of the School of Physical and Chemical Sciences is gratefully acknowledged. The Australian Research Council (ARC) is thanked for funding the instrumentation. This work was financially supported by the long-term project DKRVO 2013/02 of the Ministry of Culture of the Czech Republic (National Museum, 00023272). R. Scholz thanks to CNPq – Conselho Nacional de Desenvolvimento Científico e Tecnológico (grants No. 306287/2012-9 and No. 402852/2012-5). The downloading of the Raman spectra of fluellite from the RRUFF web site is acknowledged.

256 **References**
257

258 [1] M. A. Cooper, F. C. Hawthorne, A. C. Roberts, E. E. Foord, R. C. Erd, H. T. Evans, Jr.,

259 M. C. Jensen, Can. Min. 42 (2004) 741-752.

260 [2] J. Sejkora, R. Škoda, P. Ondruš, P. Beran, C. Süsser, J. Czech Geol. Soc. 51 (2006) 103-

261 147.

262 [3] L. E. Kearns, B. S. Martin, Virginia Min. 46 (2000), 9-16.

263 [4] H. D. Gay, R. Lira, Revista Asoc. Argen. Min. (1987) 27-32.

264 [5] K. Tazaki, W. S. Fyfe, C. B. Dissanayake, App. Geochem. 1 (1986), 287-300.

265 [6] K. Tazaki, W. S. Fyfe, C. B. Dissanayake, Chem. Geol. 60 (1987), 151-162.

266 [7] A. M. Fransolet, J. Jedwab, R. Van Tassel, Ann. Soc. Geol. Belg. 97 (1974) 27-38.

267 [8] W.A. Henderson, Jr., V. Peisley, Min. Rec.16 (1985) 477-480.

268 [9] S. Menchetti, C. Sabelli, N. Jb. Miner. Mh.1981 (1981) 505-510.

269 [10] M. C. Jensen, J. C. Rota, E. E. Foord, Min. Rec.26 (1995), 449-469.

270 [11] V. Y. Karpenko, L. A. Pautov, A. A. Agakhanov, Zap. Ross. Min. Obsh. 138 (2009) 83-

271 90.

272 [12] A. Levy, Annals Phil. 8 (1824) 241-245.

273 [13] P. Groth, Jahrb. f. Min. 2 (1883) 324-327.

274 [14] H. Laubmann, H. Steinmetz, Zeit. Krist. 55 (1920), 549-557.

275 [15] A. Scholz, H. Strunz, Geol. Pal.1940A (1940) 133-137.

276 [16] B. B. Guy, G. A. Jeffrey, Amer. Min. 51 (1966) 1579-1592.

277 [17] B. B. Guy, G. A. Jeffrey, R. Van Tassel, Amer. Min. 52 (1967) 1577.

278 [18] J. Sejkora, T. Řídkošil, V. Šrein, Zálesíite, 175 (1999) 105-124.

279 [19] J. Sejkora, F. C. Hawthorne, M. A. Cooper, J. D. Grice, J. Vajdak, J. L. Jambor, Can.

280 Min. 47 (2009) 159-164.

281 [20] J. Sejkora, K. Babka R. Pavlíček, Bull. mineral.-petrolog. Odd. Nár. Muz. (Praha) 20
282 (2012) 208-212.
283 [21] J. Sejkora, P. Pauliš, P. Rus, R. Škoda, L. Koťátko, Bull. mineral.-petrolog. Odd. Nár.
284 Muz. (Praha) 20 (2012) 177-182.
285 [22] R. L. Frost, J. Čejka, J. Sejkora, D Ozdín, S. Bahfenne, E. C. Keeffe, J. Raman
286 Spectrosc. 40 (2009) 1907-1910.
287 [23] J. Čejka, R. L. Frost, J. Sejkora, E. C. Keefee, J. Raman Spectrosc. 40 (2009) 1464-
288 1468.
289 [24] R. L. Frost, J. Sejkora, J. Čejka, E.C. Keeffe, J. Raman Spectrosc. 40 (2009) 1546-1550.
290 [25] J. Sejkora, J. Litochleb, J. Čejka, P. Černý, Bull. mineral.-petrolog. Odd. Nár. Muz.
291 (Praha) 21 (2013) 37-46.
292 [26] E. S. Pilkington, E. R. Segnit, J. A. Watts, Min. Mag. 46 (1982), 449-452.
293 [27] P. Ondruš, ZDS - software for analysis of X-ray powder diffraction patterns. Version
294 6.01. User´s guide (1995), Praha.
295 [28] C. W. Burnham, Yearb. 61 (1962), 132-135.
296 [29] Nakamoto K, Infrared and Raman spectra of inorganand coordination compounds, J.
297 Wiley and Sons New York (1986).
298 [30] Pechkovskii V.V., Mel'nikova R.Ya., Dzyuba E.D., Baranikova T.I., Nikanovich M.V.,
299 Nauka Moscow 1981 (in Russian).
300 [31] Rahten A., Benkich P., Jesih A., Acta Chim. Slov. 46, 339-354 (1999).
301 [32] D. K. Breitinger, H. H. Belz, L. Hajba, V. Komlosi, J. Mink, G. Brehm, D. Colognesi, S.
302 F. Parker, R. G. Schwab, J. Mol. Struct.706 (2004) 95-99.
303 [33] Diafi M., Omari M., Boletin de la Sociedad Española de Cerámica y Vidrio 51, 337-342
304 (2012).
305 [34] Libowitzky E., Monatshefte für Chem. 130, 1047-1059 (1999)
306

TABLES

Table 1 Unit-cell parameters of fluellite

	a [Å]	*b [Å]*	*c [Å]*	*V [Å^3]*
Krásno (CZ)	8.558(1)	11.237(1)	21.179(2)	2043.5(3)
Kapunda (AU)	8.5703(5)	11.2454(8)	21.175(1)	2040.8(1)
Cornwall [16]	8.546(8)	11.222(5)	21.158(5)	2029.12

316 Table 2 Chemical composition of fluellite from Krásno (CZ)
317

wt. %	mean 1-4	1	2	3	4	ideal**
Al_2O_3	36.40	36.98	36.32	36.23	36.06	30.89
P_2O_5	27.29	27.10	27.39	26.93	27.74	21.51
F	13.65	13.54	13.37	13.96	13.75	11.51
H_2O*	47.95	48.95	47.94	47.58	47.30	40.95
-F=O	5.75	5.70	5.63	5.88	5.79	4.86
total	119.54	120.87	119.38	118.82	119.06	100.00

318 Additional elements (Na, K, Mn, Sr, Ba, Ca, Cu, Zn, Fe, Bi, Si, As, S and Cl) were analyzed;
319 the analysis confirmed their absence or contents below detection limits (ca 0.01-0.05 wt. %).
320 H_2O* content was calculated on the basis of ideal composition; ideal** - ideal composition
321 calculated from formula $Al_2(PO_4)F_2(OH).7H_2O$.
322
323
324
325

Table 3 Tentative assignment of fluellite spectra

CZ Raman	AU Raman	AU IR	USA* Raman	Tentative assignment
3667		3629		ν OH stretch of $(OH)^-$
		3559		
	3411	3441		ν OH stretch of water molecules
3396	3356			
3314	3222	3221		
3124	3113	3047		
1670	1675	1660		δ H_2O bend
		1624		
	1603			
		1575		overtones of combination bands
1583	1503	1537		
		1224		ν_3 $(PO_4)^{3-}$ antisymmetric stretch
		1175		
1122	1123		1120	
1096	1083	1102	1096	
	1061	1061		
1036	1037	1026	1038	ν_1 $(PO_4)^{3-}$ symmetric stretch
	1003			δ Al-OH bend
	963	965		
897	926	920	910	
835			880	
646	638		651	ν_4 (δ) $(PO_4)^{3-}$ out-of-plane bend; ν $Al(O(OH)F)_6$ bend
	614			
588	588		585	
557				ν_4 (δ) $(PO_4)^{3-}$ out-of-plane bend
525	522		524	
513	510			
459			462	ν_2 (δ) $(PO_4)^{3-}$ bend
410	410		406	
	399			ν $Al(O(OH)F)_6$ stretch
	360			
342				
311			313	
295	297			O-Al-O skeletal vibrations
279	279		276	
	258			
251	249			
220				lattice vibrations
208			211	
199				
191	194			
173			173	
151	153			
139	141			
123				
116	113			
108				

USA* RRUFF spectrum (R070473) of fluellite from Gold Quarry mine, Maggie Creek District, Eureka County, Nevada (U.S.A.)

Figures

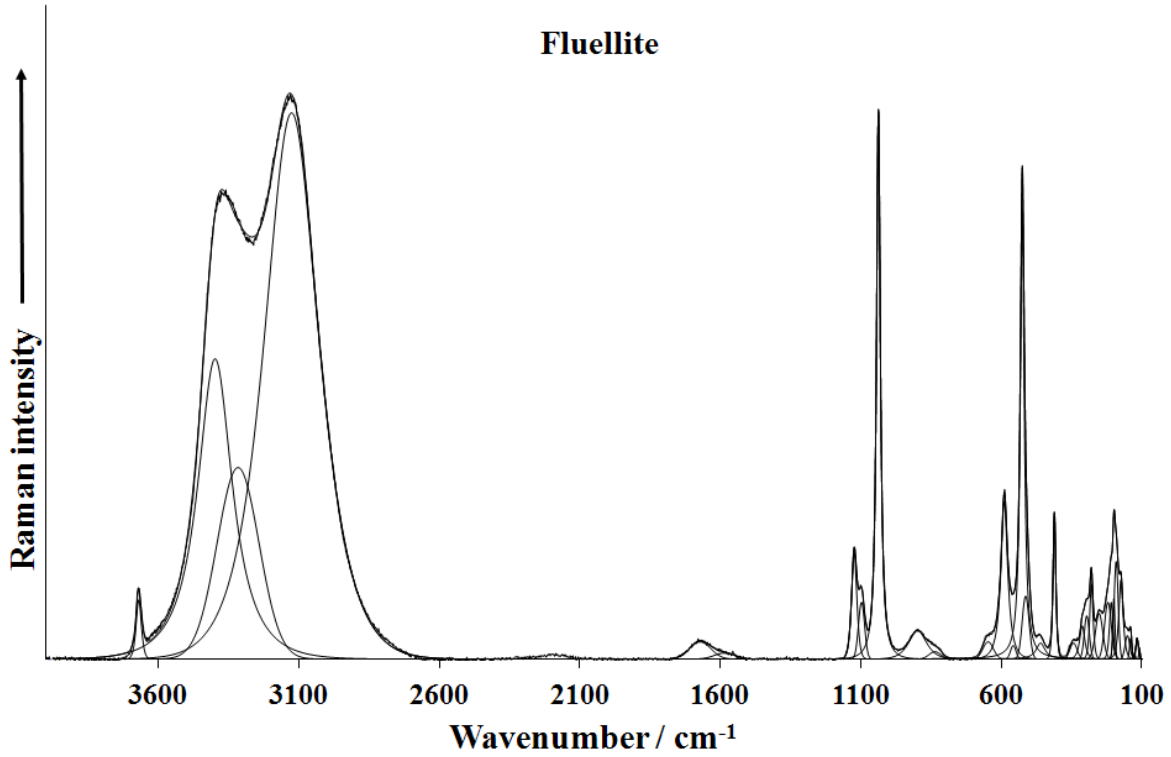

Fig. 1a Raman spectrum of fluellite sample CZ over the 100 to 4000 cm^{-1} spectral range

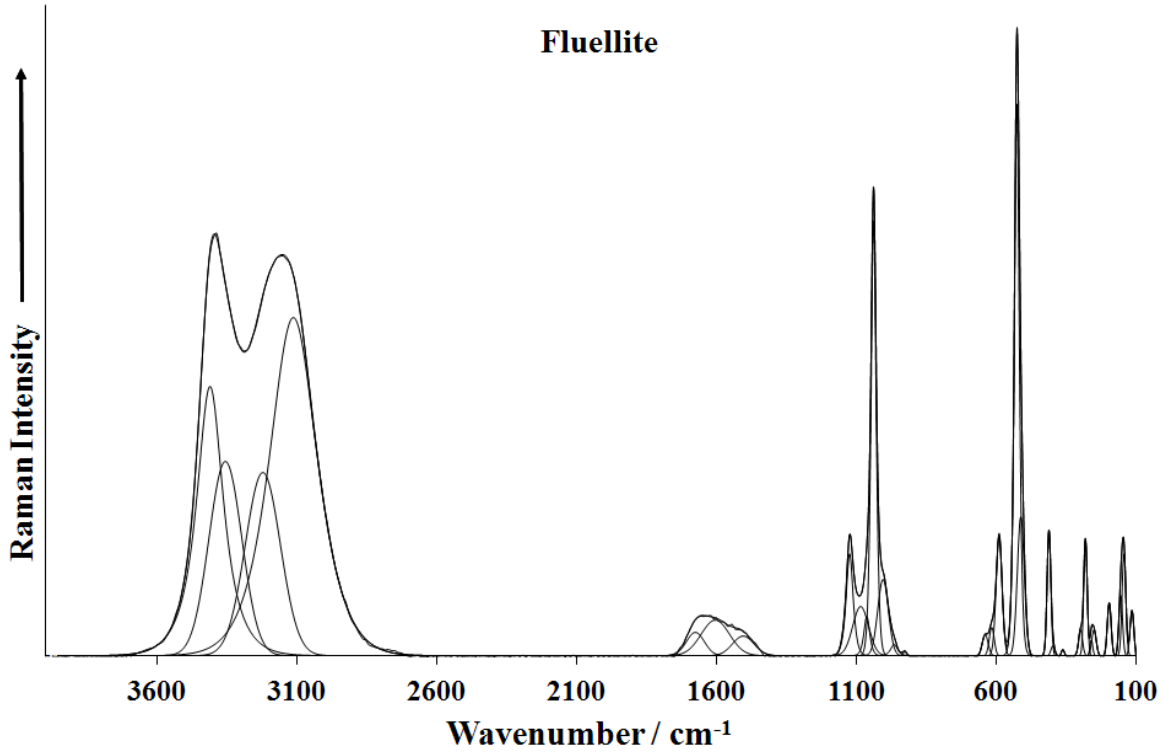

Fig. 1b Raman spectrum of fluellite sample AU over the 100 to 4000 cm^{-1} spectral range

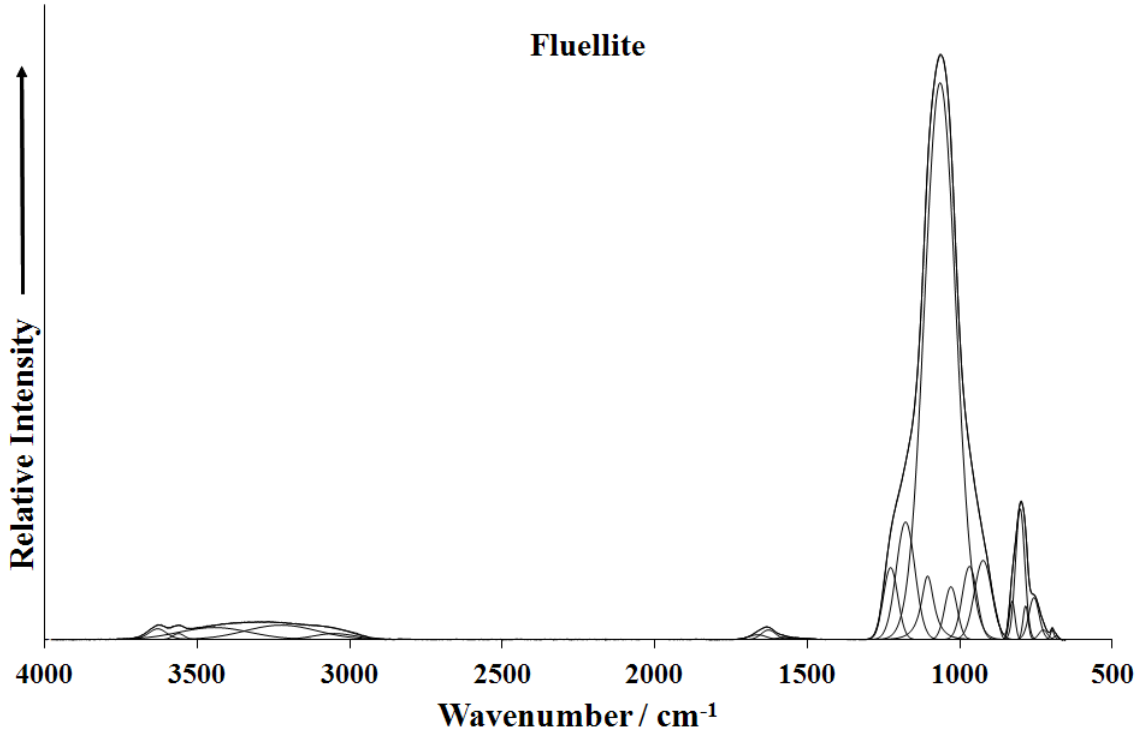

341
342
343 **Fig. 1c infrared spectra of fluellite AU over the 500 to 4000 cm^{-1} spectral range**
344
345
346
347
348

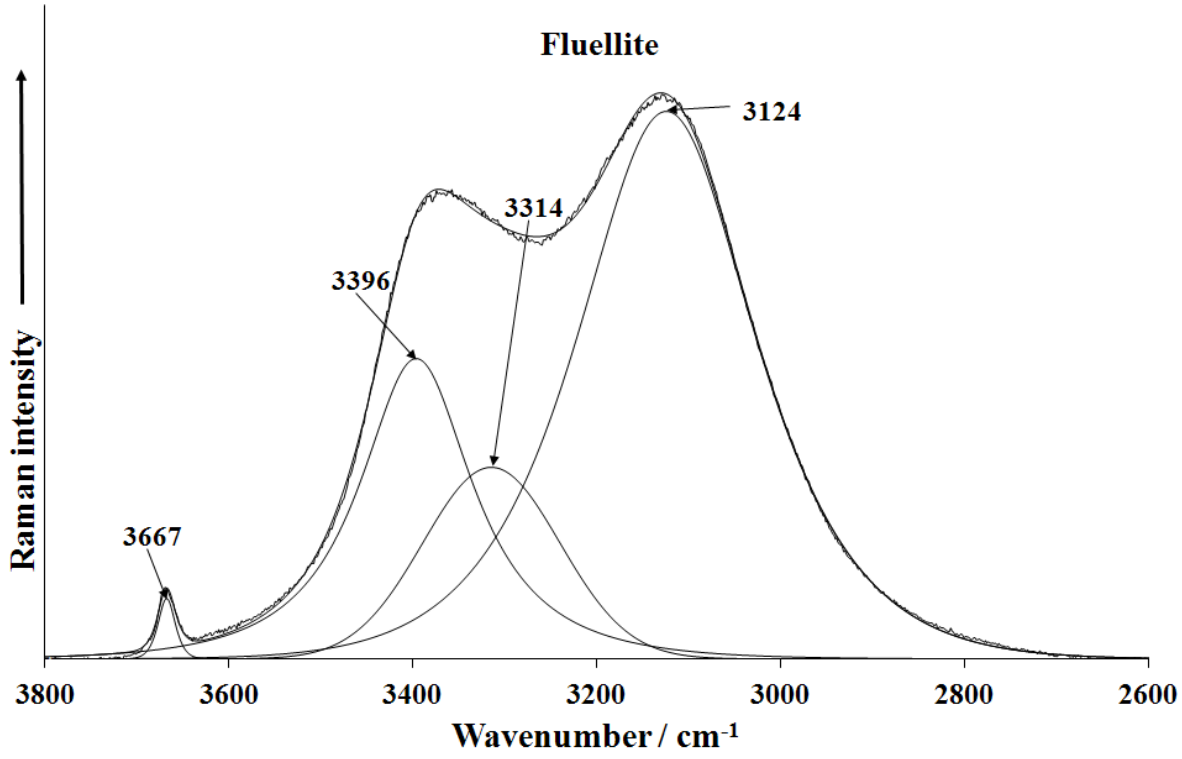

349
350 **Fig 2a Raman spectrum of fluellite CZ over the 2600 to 3800 cm^{-1} spectral range**

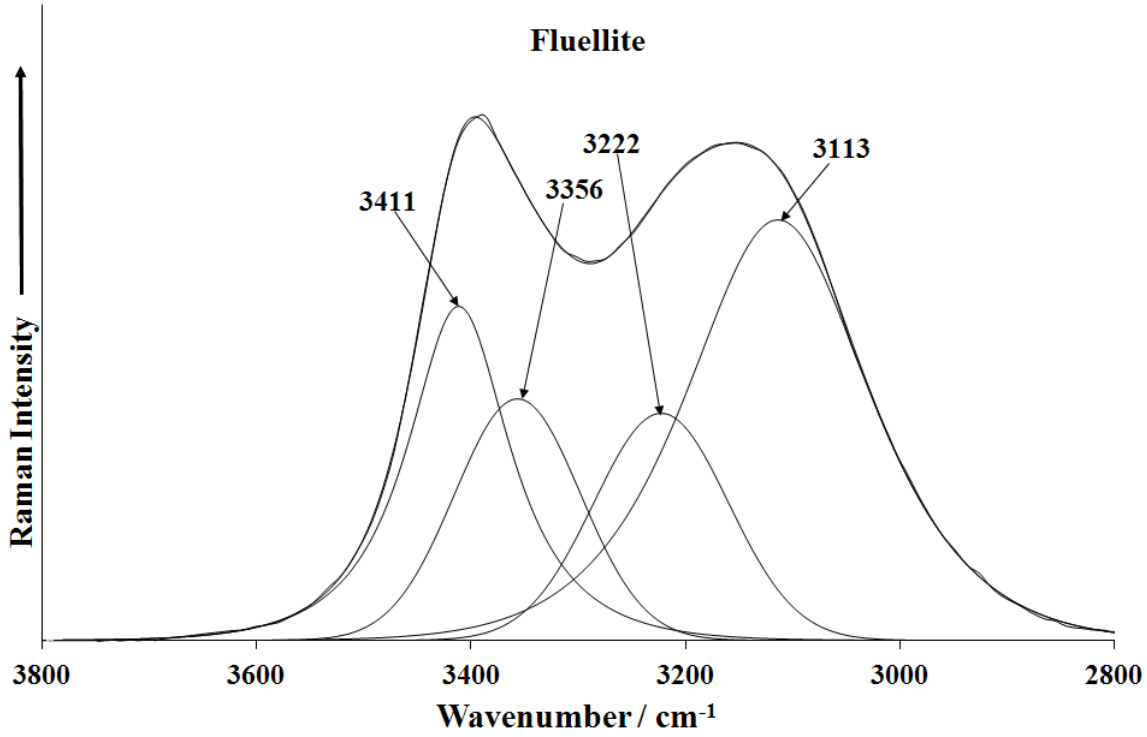

Fig 2b Raman spectrum of fluellite AU over the 2600 to 3800 cm^{-1} spectral range

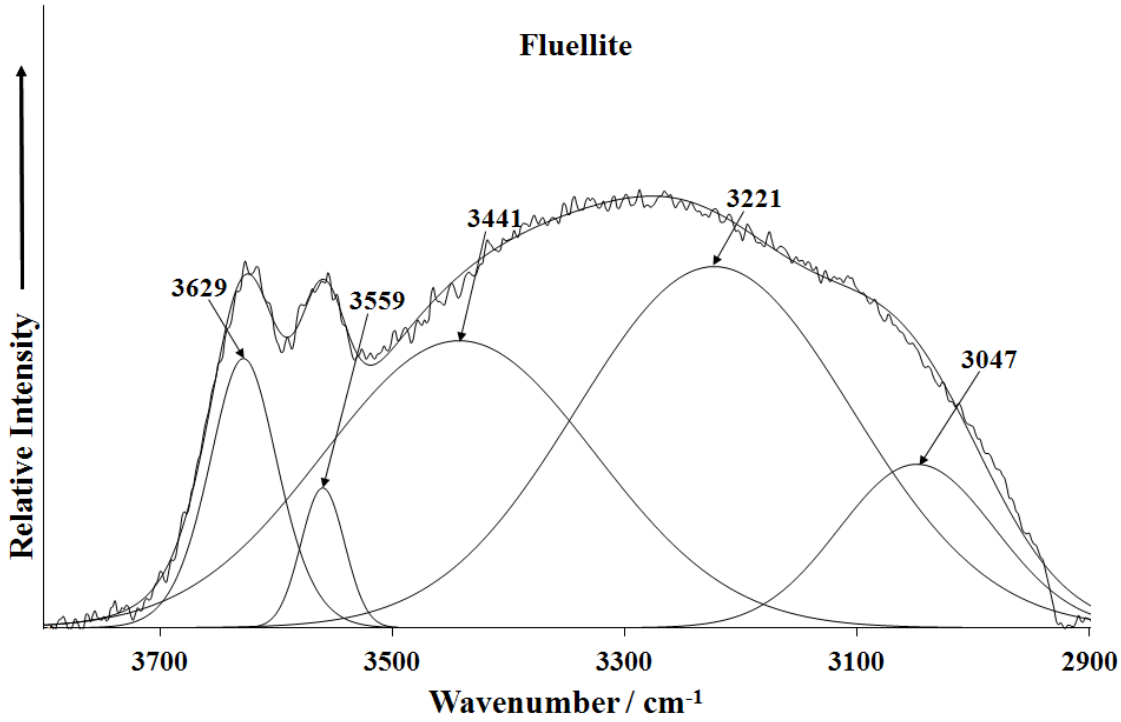

Fig. 2c Infrared spectrum of fluellite AU over the 2900 to 3800 cm^{-1} range

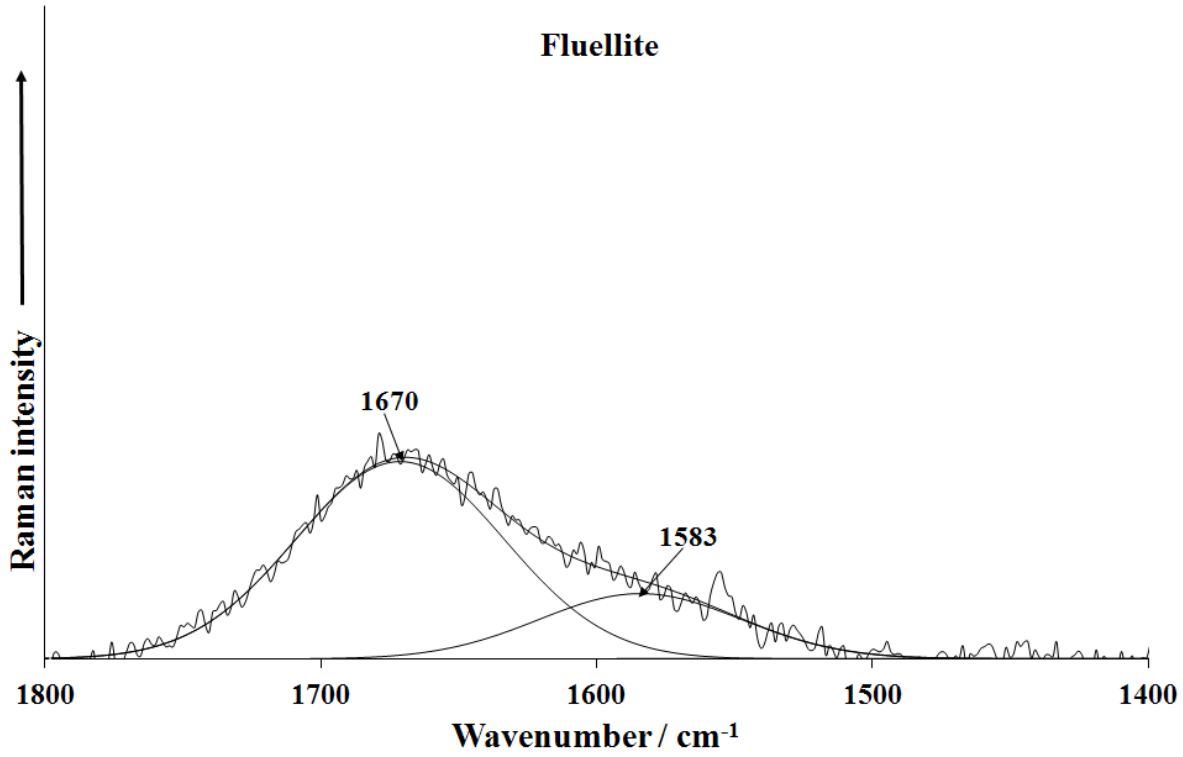

Fig. 3a Raman spectrum of fluellite CZ over the 1400 to 1800 cm^{-1} spectral range.

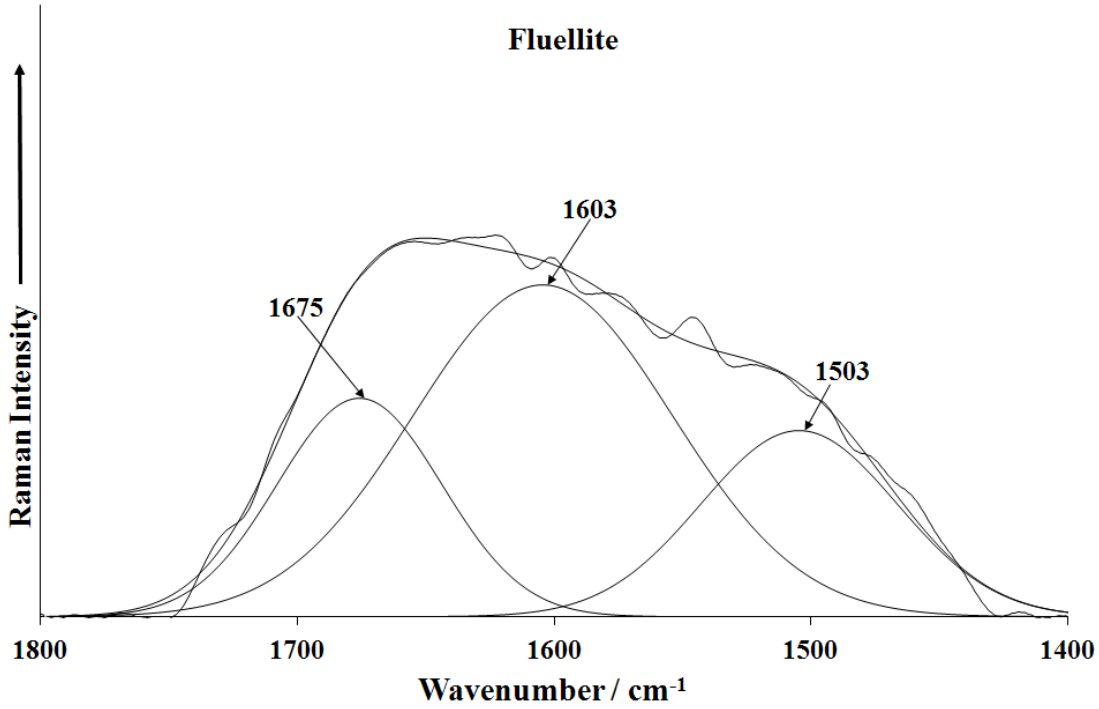

Fig. 3b Raman spectrum of fluellite AU over the 1400 to 1800 cm^{-1} spectral range.

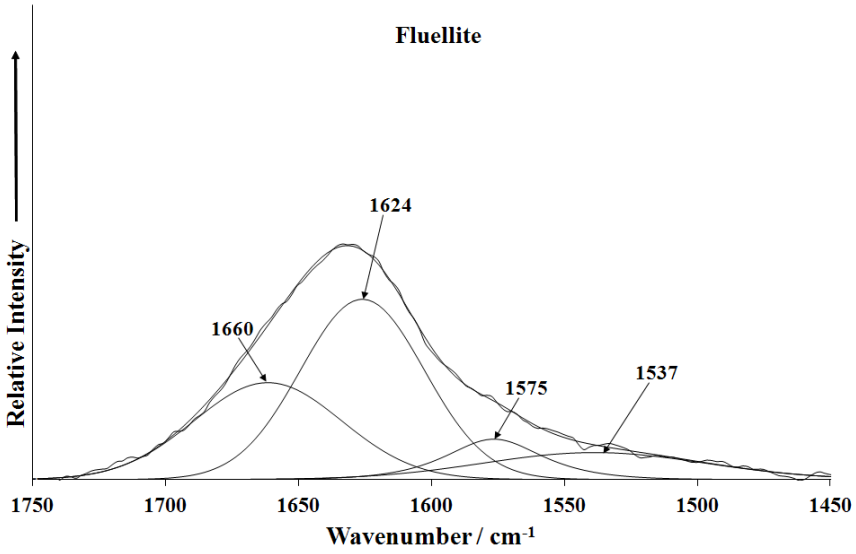

Fig. 3c Infrared spectrum of fluellite AU over the 1450 to 1750 cm^{-1} range

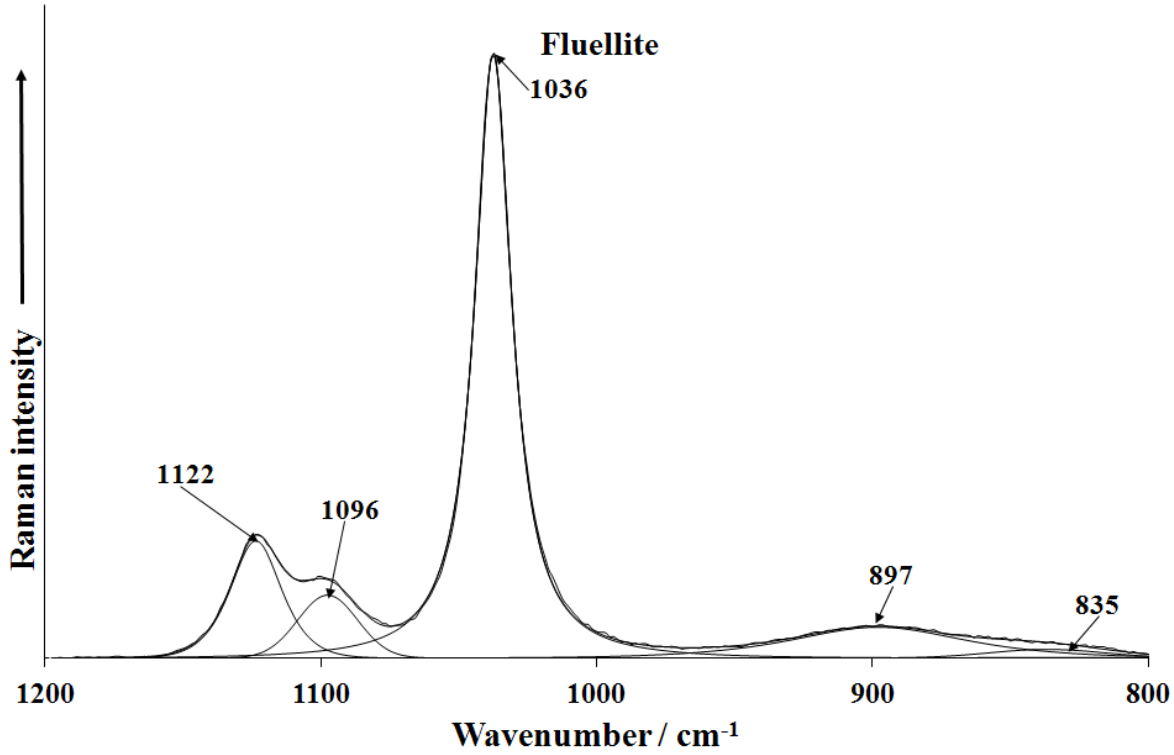

Fig. 4a Raman spectrum of fluellite CZ over the 800 to 1200 cm^{-1} range.

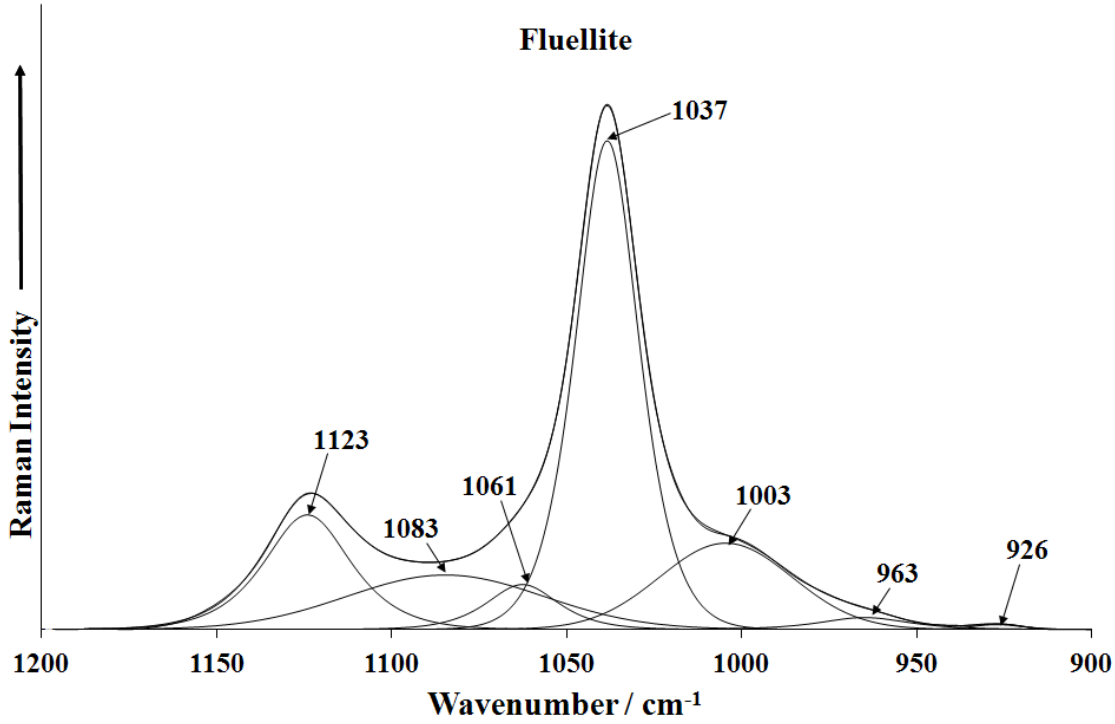

Fig. 4b Raman spectrum of fluellite AU over the 900 to 1200 cm^{-1} range.

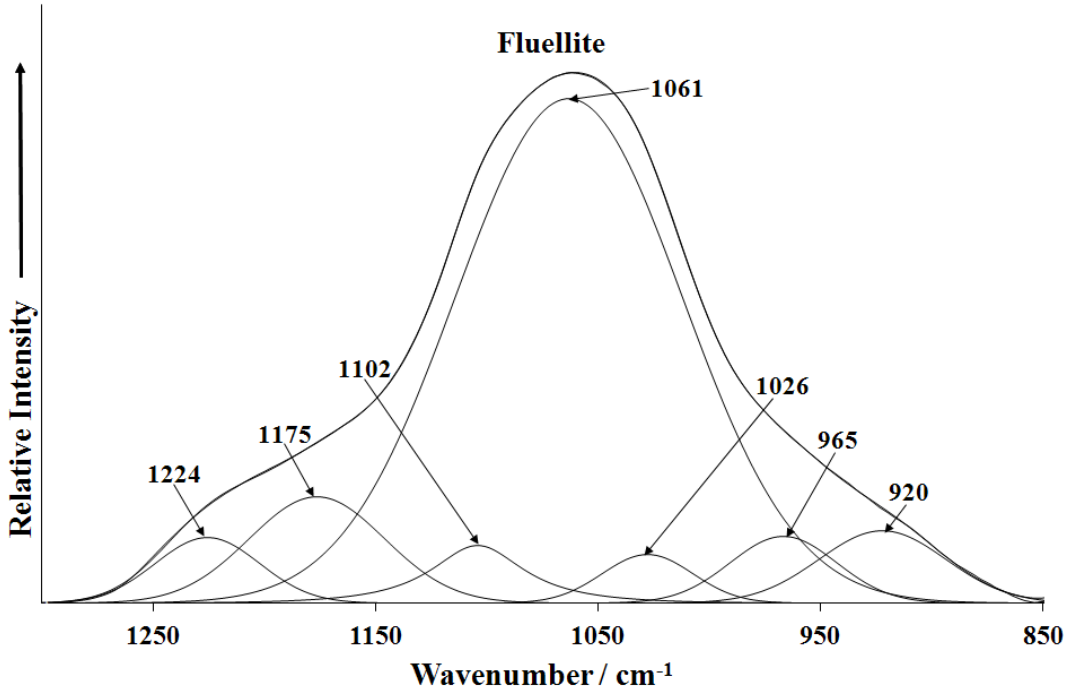

Fig. 4c Infrared spectrum of fluellite AU over the 850 to 1300 cm^{-1} range

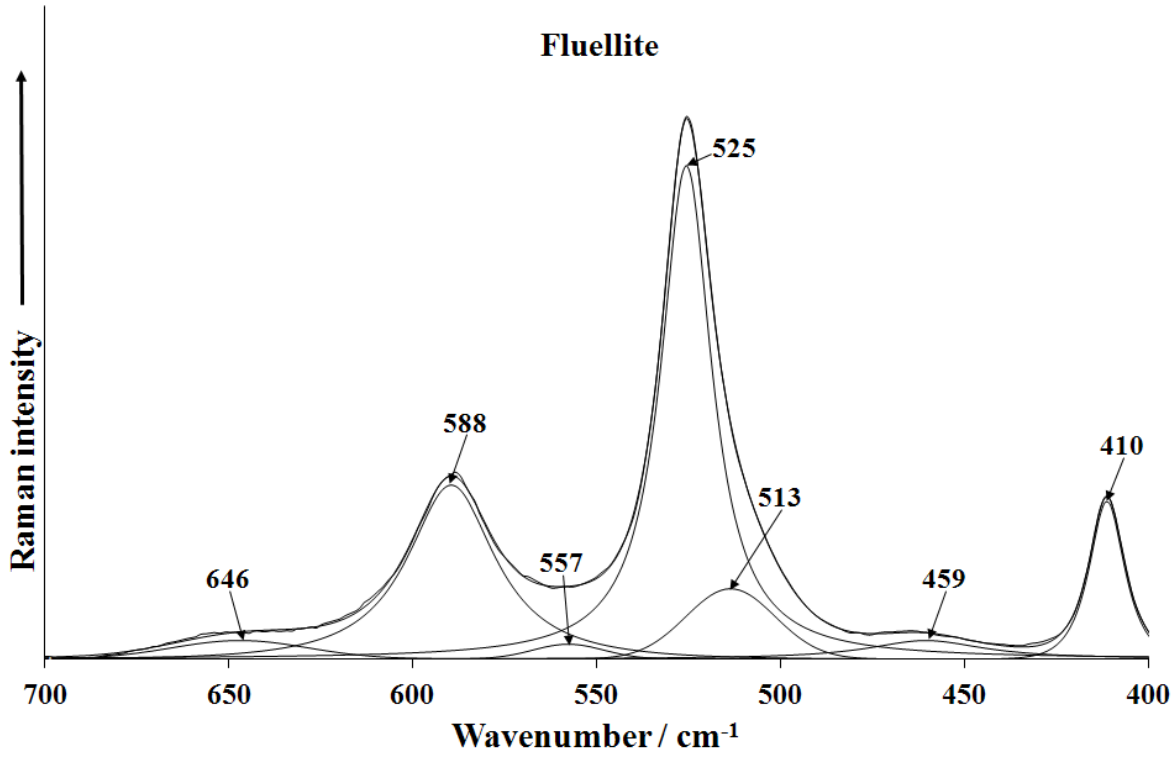

382
383
384 **Fig. 5a Raman spectrum of fluellite CZ over the 400 to 700 cm^{-1} range**
385

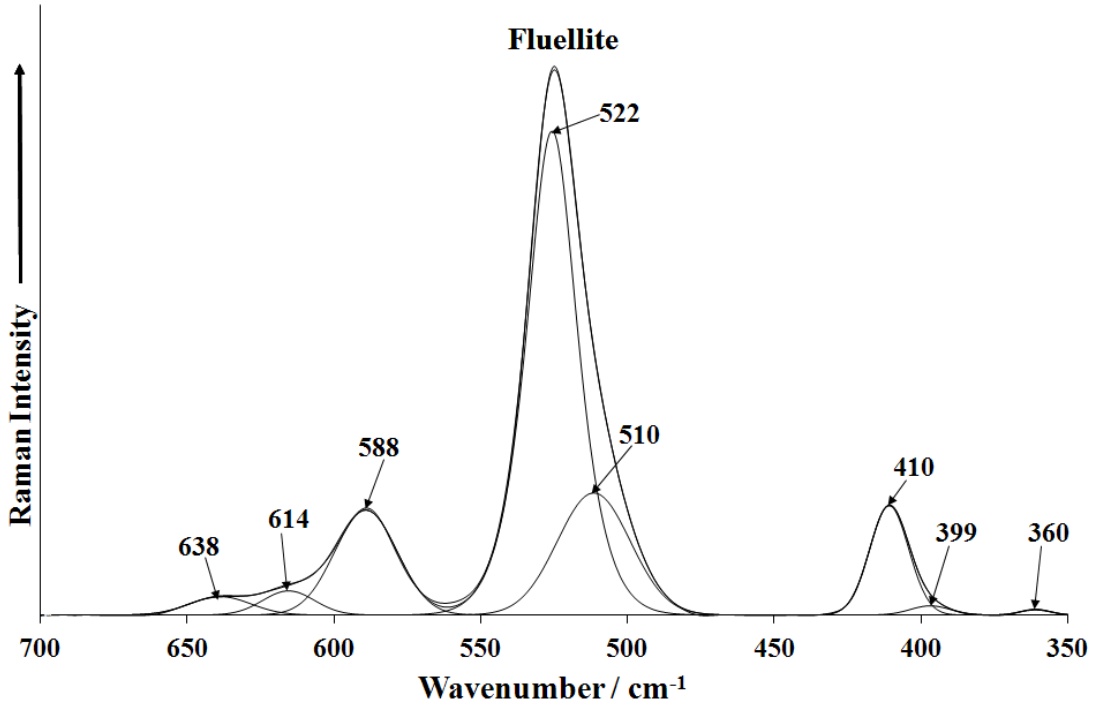

386
387
388 **Fig. 5b Raman spectrum of fluellite AU over the 350 to 700 cm^{-1} range**
389
390

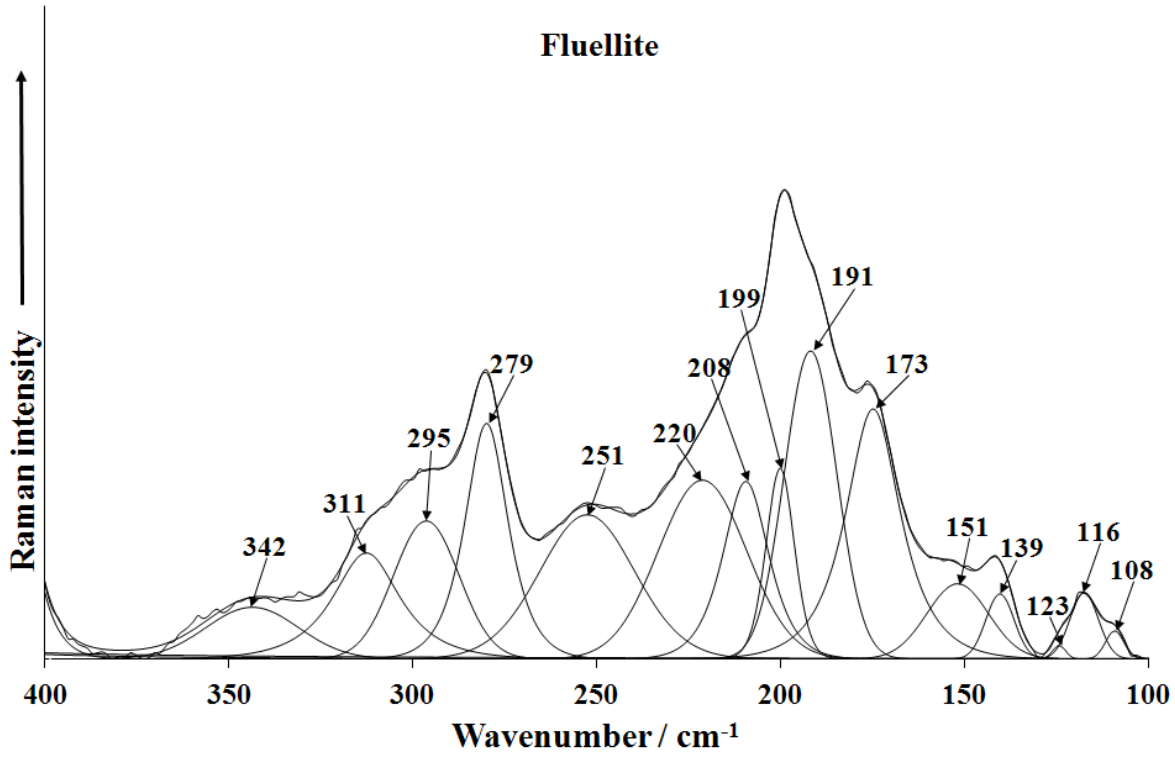

Fig. 6a Raman spectrum of fluellite CZ over the 100 to 400 cm^{-1} range.

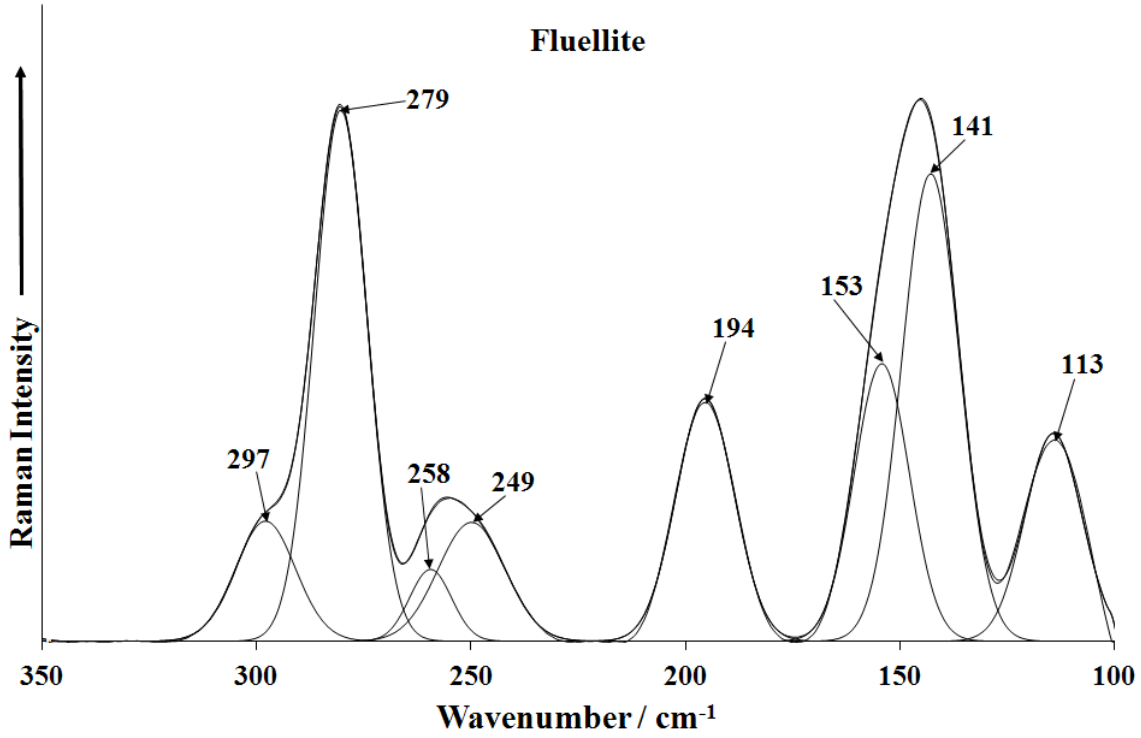

Fig. 6b Raman spectrum of fluellite AU over the 100 to 350 cm^{-1} range.

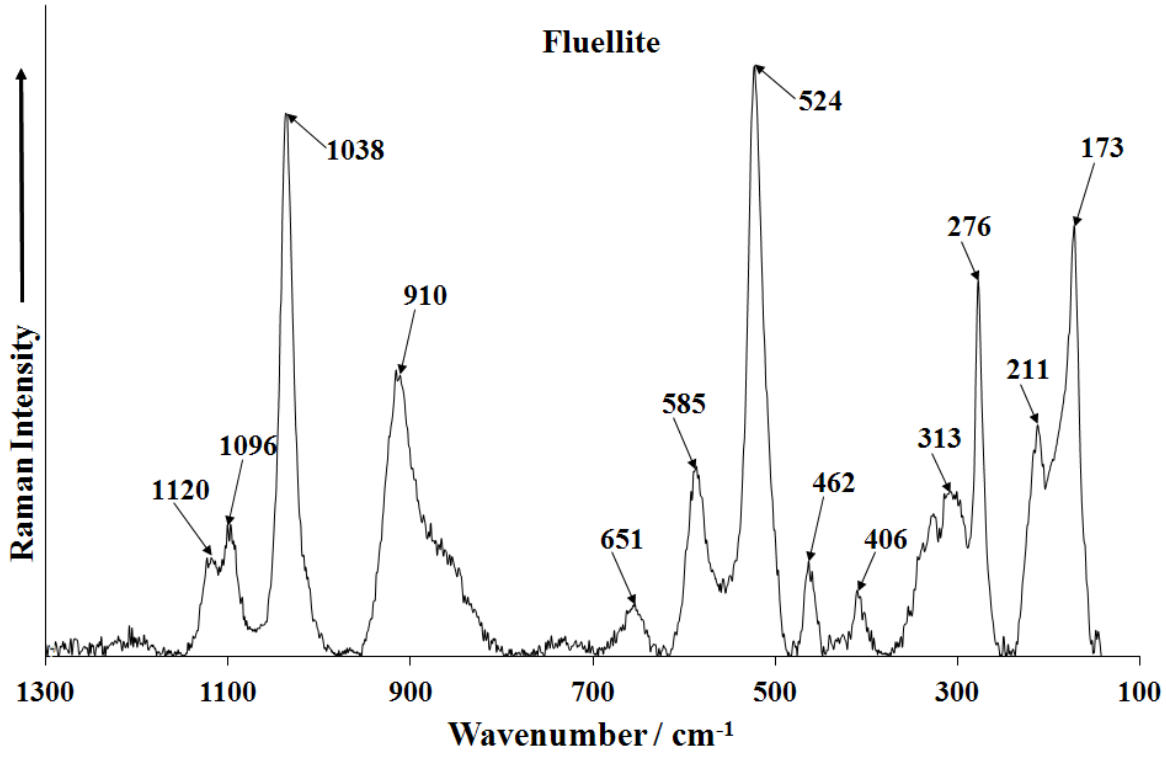

Fig. S1 Raman spectrum of fluellite from Gold Quarry mine, Maggie Creek District, Eureka County, Nevada, U.S.A. (RRUFF R070473) over the 100 to 1300 cm^{-1} range.